University of Groningen

Improved measurement of the branching fractions for J/ψ →γπ0, γη, and γη′

BESIII Collaboration; Kalantar-Nayestanaki, N.; Kavatsyuk, M.; Messchendorp, J.

IMPORTANT NOTE: You are advised to consult the publisher's version (publisher's PDF) if you wish to cite from it. Please check the document version below.

Document Version
Publisher's PDF, also known as Version of record

Publication date:
2023

[Link to publication in University of Groningen/UMCG research database](#)

Improved measurement of the branching fractions
for $J/\psi \to \gamma\pi^0$, $\gamma\eta$, and $\gamma\eta'$

M. Ablikim,[1] M. N. Achasov,[5,b] P. Adlarson,[75] X. C. Ai,[81] R. Aliberti,[36] A. Amoroso,[74a,74c] M. R. An,[40] Q. An,[71,58] Y. Bai,[57] O. Bakina,[37] I. Balossino,[30a] Y. Ban,[47,g] V. Batozskaya,[1,45] K. Begzsuren,[33] N. Berger,[36] M. Berlowski,[45] M. Bertani,[29a] D. Bettoni,[30a] F. Bianchi,[74a,74c] E. Bianco,[74a,74c] A. Bortone,[74a,74c] I. Boyko,[37] R. A. Briere,[6] A. Brueggemann,[68] H. Cai,[76] X. Cai,[1,58] A. Calcaterra,[29a] G. F. Cao,[1,63] N. Cao,[1,63] S. A. Cetin,[62a] J. F. Chang,[1,58] T. T. Chang,[77] W. L. Chang,[1,63] G. R. Che,[44] G. Chelkov,[37,a] C. Chen,[44] Chao Chen,[55] G. Chen,[1] H. S. Chen,[1,63] M. L. Chen,[1,58,63] S. J. Chen,[43] S. L. Chen,[46] S. M. Chen,[61] T. Chen,[1,63] X. R. Chen,[32,63] X. T. Chen,[1,63] Y. B. Chen,[1,58] Y. Q. Chen,[35] Z. J. Chen,[26,h] W. S. Cheng,[74c] S. K. Choi,[11] X. Chu,[44] G. Cibinetto,[30a] S. C. Coen,[4] F. Cossio,[74c] J. J. Cui,[50] H. L. Dai,[1,58] J. P. Dai,[79] A. Dbeyssi,[19] R. E. de Boer,[4] D. Dedovich,[37] Z. Y. Deng,[1] A. Denig,[36] I. Denysenko,[37] M. Destefanis,[74a,74c] F. De Mori,[74a,74c] B. Ding,[66,1] X. X. Ding,[47,g] Y. Ding,[41] Y. Ding,[35] J. Dong,[1,58] L. Y. Dong,[1,63] M. Y. Dong,[1,58,63] X. Dong,[76] M. C. Du,[1] S. X. Du,[81] Z. H. Duan,[43] P. Egorov,[37,a] Y. H. Fan,[46] Y. L. Fan,[76] J. Fang,[1,58] S. S. Fang,[1,63] W. X. Fang,[1] Y. Fang,[1] R. Farinelli,[30a] L. Fava,[74b,74c] F. Feldbauer,[4] G. Felici,[29a] C. Q. Feng,[71,58] J. H. Feng,[59] K. Fischer,[69] M. Fritsch,[4] C. Fritzsch,[68] C. D. Fu,[1] J. L. Fu,[63] Y. W. Fu,[1] H. Gao,[63] Y. N. Gao,[47,g] Yang Gao,[71,58] S. Garbolino,[74c] I. Garzia,[30a,30b] P. T. Ge,[76] Z. W. Ge,[43] C. Geng,[59] E. M. Gersabeck,[67] A. Gilman,[69] K. Goetzen,[14] L. Gong,[41] W. X. Gong,[1,58] W. Gradl,[36] S. Gramigna,[30a,30b] M. Greco,[74a,74c] M. H. Gu,[1,58] Y. T. Gu,[16] C. Y. Guan,[1,63] Z. L. Guan,[23] A. Q. Guo,[32,63] L. B. Guo,[42] M. J. Guo,[50] R. P. Guo,[49] Y. P. Guo,[13,f] A. Guskov,[37,a] T. T. Han,[50] W. Y. Han,[40] X. Q. Hao,[20] F. A. Harris,[65] K. K. He,[55] K. L. He,[1,63] F. H. H. Heinsius,[4] C. H. Heinz,[36] Y. K. Heng,[1,58,63] C. Herold,[60] T. Holtmann,[4] P. C. Hong,[13,f] G. Y. Hou,[1,63] X. T. Hou,[1,63] Y. R. Hou,[63] Z. L. Hou,[1] H. M. Hu,[1,63] J. F. Hu,[56,i] T. Hu,[1,58,63] Y. Hu,[1] G. S. Huang,[71,58] K. X. Huang,[59] L. Q. Huang,[32,63] X. T. Huang,[50] Y. P. Huang,[1] T. Hussain,[73] N. Hüsken,[28,36] W. Imoehl,[28] N. in der Wiesche,[68] M. Irshad,[71,58] J. Jackson,[28] S. Jaeger,[4] S. Janchiv,[33] J. H. Jeong,[11] Q. Ji,[1] Q. P. Ji,[20] X. B. Ji,[1,63] X. L. Ji,[1,58] Y. Y. Ji,[50] X. Q. Jia,[50] Z. K. Jia,[71,58] H. J. Jiang,[76] P. C. Jiang,[47,g] S. S. Jiang,[40] T. J. Jiang,[17] X. S. Jiang,[1,58,63] Y. Jiang,[63] J. B. Jiao,[50] Z. Jiao,[24] S. Jin,[43] Y. Jin,[66] M. Q. Jing,[1,63] T. Johansson,[75] X. K.,[1] S. Kabana,[34] N. Kalantar-Nayestanaki,[64] X. L. Kang,[10] X. S. Kang,[41] M. Kavatsyuk,[64] B. C. Ke,[81] A. Khoukaz,[68] R. Kiuchi,[1] R. Kliemt,[14] O. B. Kolcu,[62a] B. Kopf,[4] M. Kuessner,[4] A. Kupsc,[45,75] W. Kühn,[38] J. J. Lane,[67] P. Larin,[19] A. Lavania,[27] L. Lavezzi,[74a,74c] T. T. Lei,[71,58] Z. H. Lei,[71,58] H. Leithoff,[36] M. Lellmann,[36] T. Lenz,[36] C. Li,[48] C. Li,[44] C. H. Li,[40] Cheng Li,[71,58] D. M. Li,[81] F. Li,[1,58] G. Li,[1] H. Li,[71,58] H. B. Li,[1,63] H. J. Li,[20] H. N. Li,[56,i] Hui Li,[44] J. R. Li,[61] J. S. Li,[59] J. W. Li,[50] K. L. Li,[20] Ke Li,[1] L. J. Li,[1,63] L. K. Li,[1] Lei Li,[3] M. H. Li,[44] P. R. Li,[39,j,k] Q. X. Li,[50] S. X. Li,[13] T. Li,[50] W. D. Li,[1,63] W. G. Li,[1] X. H. Li,[71,58] X. L. Li,[50] Xiaoyu Li,[1,63] Y. G. Li,[47,g] Z. J. Li,[59] Z. X. Li,[16] C. Liang,[43] H. Liang,[35] H. Liang,[71,58] H. Liang,[1,63] Y. F. Liang,[54] Y. T. Liang,[32,63] G. R. Liao,[15] L. Z. Liao,[50] Y. P. Liao,[1,63] J. Libby,[27] A. Limphirat,[60] D. X. Lin,[32,63] T. Lin,[1] B. J. Liu,[1] B. X. Liu,[76] C. Liu,[35] C. X. Liu,[1] F. H. Liu,[53] Fang Liu,[1] Feng Liu,[7] G. M. Liu,[56,i] H. Liu,[39,j,k] H. B. Liu,[16] H. M. Liu,[1,63] Huanhuan Liu,[1] Huihui Liu,[22] J. B. Liu,[71,58] J. L. Liu,[72] J. Y. Liu,[1,63] K. Liu,[1] K. Y. Liu,[41] Ke Liu,[23] L. Liu,[71,58] L. C. Liu,[44] Lu Liu,[44] M. H. Liu,[13,f] P. L. Liu,[1] Q. Liu,[63] S. B. Liu,[71,58] T. Liu,[13,f] W. K. Liu,[44] W. M. Liu,[71,58] X. Liu,[39,j,k] Y. Liu,[81] Y. Liu,[39,j,k] Y. B. Liu,[44] Z. A. Liu,[1,58,63] Z. Q. Liu,[50] X. C. Lou,[1,58,63] F. X. Lu,[59] H. J. Lu,[24] J. G. Lu,[1,58] X. L. Lu,[1] Y. Lu,[8] Y. P. Lu,[1,58] Z. H. Lu,[1,63] C. L. Luo,[42] M. X. Luo,[80] T. Luo,[13,f] X. L. Luo,[1,58] X. R. Lyu,[63] Y. F. Lyu,[44] F. C. Ma,[41] H. L. Ma,[1] J. L. Ma,[1,63] L. L. Ma,[50] M. M. Ma,[1,63] Q. M. Ma,[1] R. Q. Ma,[1,63] R. T. Ma,[63] X. Y. Ma,[1,58] Y. Ma,[47,g] Y. M. Ma,[32] F. E. Maas,[19] M. Maggiora,[74a,74c] S. Malde,[69] Q. A. Malik,[73] A. Mangoni,[29b] Y. J. Mao,[47,g] Z. P. Mao,[1] S. Marcello,[74a,74c] Z. X. Meng,[66] J. G. Messchendorp,[14,64] G. Mezzadri,[30a] H. Miao,[1,63] T. J. Min,[43] R. E. Mitchell,[28] X. H. Mo,[1,58,63] N. Yu. Muchnoi,[5,b] J. Muskalla,[36] Y. Nefedov,[37] F. Nerling,[19,d] I. B. Nikolaev,[5,b] Z. Ning,[1,58] S. Nisar,[12,l] Y. Niu,[50] S. L. Olsen,[63] Q. Ouyang,[1,58,63] S. Pacetti,[29b,29c] X. Pan,[55] Y. Pan,[57] A. Pathak,[35] P. Patteri,[29a] Y. P. Pei,[71,58] M. Pelizaeus,[4] H. P. Peng,[71,58] K. Peters,[14,d] J. L. Ping,[42] R. G. Ping,[1,63] S. Plura,[36] S. Pogodin,[37] V. Prasad,[34] F. Z. Qi,[1] H. Qi,[71,58] H. R. Qi,[61] M. Qi,[43] T. Y. Qi,[13,f] S. Qian,[1,58] W. B. Qian,[63] C. F. Qiao,[63] J. J. Qin,[72] L. Q. Qin,[15] X. P. Qin,[13,f] X. S. Qin,[50] Z. H. Qin,[1,58] J. F. Qiu,[1] S. Q. Qu,[61] C. F. Redmer,[36] K. J. Ren,[40] A. Rivetti,[74c] M. Rolo,[74c] G. Rong,[1,63] Ch. Rosner,[19] S. N. Ruan,[44] N. Salone,[45] A. Sarantsev,[37,c] Y. Schelhaas,[36] K. Schoenning,[75] M. Scodeggio,[30a,30b] K. Y. Shan,[13,f] W. Shan,[25] X. Y. Shan,[71,58] J. F. Shangguan,[55] L. G. Shao,[1,63] M. Shao,[71,58] C. P. Shen,[13,f] H. F. Shen,[1,63] W. H. Shen,[63] X. Y. Shen,[1,63] B. A. Shi,[63] H. C. Shi,[71,58] J. L. Shi,[13] J. Y. Shi,[1] Q. Q. Shi,[55] R. S. Shi,[1,63] X. Shi,[1,58] J. J. Song,[20] T. Z. Song,[59] W. M. Song,[35,1] Y. J. Song,[13] Y. X. Song,[47,g] S. Sosio,[74a,74c] S. Spataro,[74a,74c] F. Stieler,[36] Y. J. Su,[63] G. B. Sun,[76] G. X. Sun,[1] H. Sun,[63] H. K. Sun,[1] J. F. Sun,[20] K. Sun,[61] L. Sun,[76] S. S. Sun,[1,63] T. Sun,[1,63] W. Y. Sun,[35] Y. Sun,[10] Y. J. Sun,[71,58] Y. Z. Sun,[1] Z. T. Sun,[50] Y. X. Tan,[71,58] C. J. Tang,[54] G. Y. Tang,[1] J. Tang,[59] Y. A. Tang,[76] L. Y. Tao,[72] Q. T. Tao,[26,h] M. Tat,[69] J. X. Teng,[71,58] V. Thoren,[75] W. H. Tian,[59] W. H. Tian,[52] Y. Tian,[32,63] Z. F. Tian,[76] I. Uman,[62b] S. J. Wang,[50] B. Wang,[1] B. L. Wang,[63] Bo Wang,[71,58] C. W. Wang,[43] D. Y. Wang,[47,g] F. Wang,[72] H. J. Wang,[39,j,k] H. P. Wang,[1,63] J. P. Wang,[50] K. Wang,[1,58] L. L. Wang,[1] M. Wang,[50] Meng Wang,[1,63] S. Wang,[39,j,k] S. Wang,[13,f] T. Wang,[13,f] T. J. Wang,[44] W. Wang,[72] W. Wang,[59] W. P. Wang,[71,58] X. Wang,[47,g] X. F. Wang,[39,j,k]

X. J. Wang,[40] X. L. Wang,[13,f] Y. Wang,[61] Y. D. Wang,[46] Y. F. Wang,[1,58,63] Y. H. Wang,[48] Y. N. Wang,[46] Y. Q. Wang,[1] Yaqian Wang,[18,1] Yi Wang,[61] Z. Wang,[1,58] Z. L. Wang,[72] Z. Y. Wang,[1,63] Ziyi Wang,[63] D. Wei,[70] D. H. Wei,[15] F. Weidner,[68] S. P. Wen,[1] C. W. Wenzel,[4] U. Wiedner,[4] G. Wilkinson,[69] M. Wolke,[75] L. Wollenberg,[4] C. Wu,[40] J. F. Wu,[1,63] L. H. Wu,[1] L. J. Wu,[1,63] X. Wu,[13,f] X. H. Wu,[35] Y. Wu,[71] Y. J. Wu,[32] Z. Wu,[1,58] L. Xia,[71,58] X. M. Xian,[40] T. Xiang,[47,g] D. Xiao,[39,j,k] G. Y. Xiao,[43] S. Y. Xiao,[1] Y. L. Xiao,[13,f] Z. J. Xiao,[42] C. Xie,[43] X. H. Xie,[47,g] Y. Xie,[50] Y. G. Xie,[1,58] Y. H. Xie,[7] Z. P. Xie,[71,58] T. Y. Xing,[1,63] C. F. Xu,[1,63] C. J. Xu,[59] G. F. Xu,[1] H. Y. Xu,[66] Q. J. Xu,[17] Q. N. Xu,[31] W. Xu,[1,63] W. L. Xu,[66] X. P. Xu,[55] Y. C. Xu,[78] Z. P. Xu,[43] Z. S. Xu,[63] F. Yan,[13,f] L. Yan,[13,f] W. B. Yan,[71,58] W. C. Yan,[81] X. Q. Yan,[1] H. J. Yang,[51,e] H. L. Yang,[35] H. X. Yang,[1] Tao Yang,[1] Y. Yang,[13,f] Y. F. Yang,[44] Y. X. Yang,[1,63] Yifan Yang,[1,63] Z. W. Yang,[39,j,k] Z. P. Yao,[50] M. Ye,[1,58] M. H. Ye,[9] J. H. Yin,[1] Z. Y. You,[59] B. X. Yu,[1,58,63] C. X. Yu,[44] G. Yu,[1,63] J. S. Yu,[26,h] T. Yu,[72] X. D. Yu,[47,g] C. Z. Yuan,[1,63] L. Yuan,[2] S. C. Yuan,[1] X. Q. Yuan,[1] Y. Yuan,[1,63] Z. Y. Yuan,[59] C. X. Yue,[40] A. A. Zafar,[73] F. R. Zeng,[50] X. Zeng,[13,f] Y. Zeng,[26,h] Y. J. Zeng,[1,63] X. Y. Zhai,[35] Y. C. Zhai,[50] Y. H. Zhan,[59] A. Q. Zhang,[1,63] B. L. Zhang,[1,63] B. X. Zhang,[1] D. H. Zhang,[44] G. Y. Zhang,[20] H. Zhang,[71] H. H. Zhang,[35] H. H. Zhang,[59] H. Q. Zhang,[1,58,63] H. Y. Zhang,[1,58] J. Zhang,[81] J. J. Zhang,[52] J. L. Zhang,[21] J. Q. Zhang,[42] J. W. Zhang,[1,58,63] J. X. Zhang,[39,j,k] J. Y. Zhang,[1] J. Z. Zhang,[1,63] Jianyu Zhang,[63] Jiawei Zhang,[1,63] L. M. Zhang,[61] L. Q. Zhang,[59] Lei Zhang,[43] P. Zhang,[1,63] Q. Y. Zhang,[40,81] Shuihan Zhang,[1,63] Shulei Zhang,[26,h] X. D. Zhang,[46] X. M. Zhang,[1] X. Y. Zhang,[50] Xuyan Zhang,[55] Y. Zhang,[72] Y. Zhang,[69] Y. T. Zhang,[81] Y. H. Zhang,[1,58] Yan Zhang,[71,58] Yao Zhang,[1] Z. H. Zhang,[1] Z. L. Zhang,[35] Z. Y. Zhang,[44] Z. Y. Zhang,[76] G. Zhao,[1] J. Zhao,[40] J. Y. Zhao,[1,63] J. Z. Zhao,[1,58] Lei Zhao,[71,58] Ling Zhao,[1] M. G. Zhao,[44] S. J. Zhao,[81] Y. B. Zhao,[1,58] Y. X. Zhao,[32,63] Z. G. Zhao,[71,58] A. Zhemchugov,[37,a] B. Zheng,[72] J. P. Zheng,[1,58] W. J. Zheng,[1,63] Y. H. Zheng,[63] B. Zhong,[42] X. Zhong,[59] H. Zhou,[50] L. P. Zhou,[1,63] X. Zhou,[76] X. K. Zhou,[7] X. R. Zhou,[71,58] X. Y. Zhou,[40] Y. Z. Zhou,[13,f] J. Zhu,[44] K. Zhu,[1] K. J. Zhu,[1,58,63] L. Zhu,[35] L. X. Zhu,[63] S. H. Zhu,[70] S. Q. Zhu,[43] T. J. Zhu,[13,f] W. J. Zhu,[13,f] Y. C. Zhu,[71,58] Z. A. Zhu,[1,63] J. H. Zou,[1] and J. Zu[71,58]

(BESIII Collaboration)

[1] *Institute of High Energy Physics, Beijing 100049, People's Republic of China*
[2] *Beihang University, Beijing 100191, People's Republic of China*
[3] *Beijing Institute of Petrochemical Technology, Beijing 102617, People's Republic of China*
[4] *Bochum Ruhr-University, D-44780 Bochum, Germany*
[5] *Budker Institute of Nuclear Physics SB RAS (BINP), Novosibirsk 630090, Russia*
[6] *Carnegie Mellon University, Pittsburgh, Pennsylvania 15213, USA*
[7] *Central China Normal University, Wuhan 430079, People's Republic of China*
[8] *Central South University, Changsha 410083, People's Republic of China*
[9] *China Center of Advanced Science and Technology,*
Beijing 100190, People's Republic of China
[10] *China University of Geosciences, Wuhan 430074, People's Republic of China*
[11] *Chung-Ang University, Seoul 06974, Republic of Korea*
[12] *COMSATS University Islamabad, Lahore Campus, Defence Road,*
Off Raiwind Road, 54000 Lahore, Pakistan
[13] *Fudan University, Shanghai 200433, People's Republic of China*
[14] *GSI Helmholtzcentre for Heavy Ion Research GmbH, D-64291 Darmstadt, Germany*
[15] *Guangxi Normal University, Guilin 541004, People's Republic of China*
[16] *Guangxi University, Nanning 530004, People's Republic of China*
[17] *Hangzhou Normal University, Hangzhou 310036, People's Republic of China*
[18] *Hebei University, Baoding 071002, People's Republic of China*
[19] *Helmholtz Institute Mainz, Staudinger Weg 18, D-55099 Mainz, Germany*
[20] *Henan Normal University, Xinxiang 453007, People's Republic of China*
[21] *Henan University, Kaifeng 475004, People's Republic of China*
[22] *Henan University of Science and Technology,*
Luoyang 471003, People's Republic of China
[23] *Henan University of Technology, Zhengzhou 450001, People's Republic of China*
[24] *Huangshan College, Huangshan 245000, People's Republic of China*
[25] *Hunan Normal University, Changsha 410081, People's Republic of China*
[26] *Hunan University, Changsha 410082, People's Republic of China*
[27] *Indian Institute of Technology Madras, Chennai 600036, India*
[28] *Indiana University, Bloomington, Indiana 47405, USA*
[29a] *INFN Laboratori Nazionali di Frascati, I-00044, Frascati, Italy*
[29b] *INFN Sezione di Perugia, I-06100, Perugia, Italy*
[29c] *University of Perugia, I-06100, Perugia, Italy*

[30a]*INFN Sezione di Ferrara, I-44122, Ferrara, Italy*
[30b]*University of Ferrara, I-44122, Ferrara, Italy*
[31]*Inner Mongolia University, Hohhot 010021, People's Republic of China*
[32]*Institute of Modern Physics, Lanzhou 730000, People's Republic of China*
[33]*Institute of Physics and Technology, Peace Avenue 54B, Ulaanbaatar 13330, Mongolia*
[34]*Instituto de Alta Investigación, Universidad de Tarapacá, Casilla 7D, Arica 1000000, Chile*
[35]*Jilin University, Changchun 130012, People's Republic of China*
[36]*Johannes Gutenberg University of Mainz, Johann-Joachim-Becher-Weg 45, D-55099 Mainz, Germany*
[37]*Joint Institute for Nuclear Research, 141980 Dubna, Moscow region, Russia*
[38]*Justus-Liebig-Universitaet Giessen, II. Physikalisches Institut,*
Heinrich-Buff-Ring 16, D-35392 Giessen, Germany
[39]*Lanzhou University, Lanzhou 730000, People's Republic of China*
[40]*Liaoning Normal University, Dalian 116029, People's Republic of China*
[41]*Liaoning University, Shenyang 110036, People's Republic of China*
[42]*Nanjing Normal University, Nanjing 210023, People's Republic of China*
[43]*Nanjing University, Nanjing 210093, People's Republic of China*
[44]*Nankai University, Tianjin 300071, People's Republic of China*
[45]*National Centre for Nuclear Research, Warsaw 02-093, Poland*
[46]*North China Electric Power University, Beijing 102206, People's Republic of China*
[47]*Peking University, Beijing 100871, People's Republic of China*
[48]*Qufu Normal University, Qufu 273165, People's Republic of China*
[49]*Shandong Normal University, Jinan 250014, People's Republic of China*
[50]*Shandong University, Jinan 250100, People's Republic of China*
[51]*Shanghai Jiao Tong University, Shanghai 200240, People's Republic of China*
[52]*Shanxi Normal University, Linfen 041004, People's Republic of China*
[53]*Shanxi University, Taiyuan 030006, People's Republic of China*
[54]*Sichuan University, Chengdu 610064, People's Republic of China*
[55]*Soochow University, Suzhou 215006, People's Republic of China*
[56]*South China Normal University, Guangzhou 510006, People's Republic of China*
[57]*Southeast University, Nanjing 211100, People's Republic of China*
[58]*State Key Laboratory of Particle Detection and Electronics,*
Beijing 100049, Hefei 230026, People's Republic of China
[59]*Sun Yat-Sen University, Guangzhou 510275, People's Republic of China*
[60]*Suranaree University of Technology,*
University Avenue 111, Nakhon Ratchasima 30000, Thailand
[61]*Tsinghua University, Beijing 100084, People's Republic of China*
[62a]*Turkish Accelerator Center Particle Factory Group, Istinye University,*
34010, Istanbul, Turkey
[62b]*Near East University, Nicosia, North Cyprus, 99138, Mersin 10, Turkey*
[63]*University of Chinese Academy of Sciences, Beijing 100049, People's Republic of China*
[64]*University of Groningen, NL-9747 AA Groningen, The Netherlands*
[65]*University of Hawaii, Honolulu, Hawaii 96822, USA*
[66]*University of Jinan, Jinan 250022, People's Republic of China*
[67]*University of Manchester, Oxford Road, Manchester M13 9PL, United Kingdom*
[68]*University of Muenster, Wilhelm-Klemm-Strasse 9, 48149 Muenster, Germany*
[69]*University of Oxford, Keble Road, Oxford OX13RH, United Kingdom*
[70]*University of Science and Technology Liaoning,*
Anshan 114051, People's Republic of China
[71]*University of Science and Technology of China,*
Hefei 230026, People's Republic of China
[72]*University of South China, Hengyang 421001, People's Republic of China*
[73]*University of the Punjab, Lahore-54590, Pakistan*
[74a]*University of Turin and INFN, University of Turin, I-10125, Turin, Italy*
[74b]*University of Eastern Piedmont, I-15121, Alessandria, Italy*
[74c]*INFN, I-10125, Turin, Italy*
[75]*Uppsala University, Box 516, SE-75120 Uppsala, Sweden*
[76]*Wuhan University, Wuhan 430072, People's Republic of China*
[77]*Xinyang Normal University, Xinyang 464000, People's Republic of China*
[78]*Yantai University, Yantai 264005, People's Republic of China*
[79]*Yunnan University, Kunming 650500, People's Republic of China*

^{80}*Zhejiang University, Hangzhou 310027, People's Republic of China*
^{81}*Zhengzhou University, Zhengzhou 450001, People's Republic of China*

Using a data sample of $(1.0087 \pm 0.0044) \times 10^{10}$ J/ψ events collected with the BESIII detector, the decays of $J/\psi \to \gamma\pi^0(\eta, \eta') \to \gamma\gamma\gamma$ are studied. Newly measured branching fractions are $\mathcal{B}(J/\psi \to \gamma\pi^0) = (3.34 \pm 0.02 \pm 0.09) \times 10^{-5}$, $\mathcal{B}(J/\psi \to \gamma\eta) = (1.096 \pm 0.001 \pm 0.019) \times 10^{-3}$, and $\mathcal{B}(J/\psi \to \gamma\eta') = (5.40 \pm 0.01 \pm 0.11) \times 10^{-3}$, where the first uncertainties are statistical and the second are systematic. These results are consistent with the world average values within two standard deviations. The ratio of partial widths $\Gamma(J/\psi \to \gamma\eta')/\Gamma(J/\psi \to \gamma\eta)$ is measured to be 4.93 ± 0.13. The singlet-octet pseudoscalar mixing angle θ_P is determined to be $\theta_P = -(22.11 \pm 0.26)°$ or $-(19.34 \pm 0.34)°$ with two different phenomenological models.

I. INTRODUCTION

Within the framework of quantum chromodynamics, the Okubo-Zweig-Iizuka-forbidden radiative decays of $J/\psi \to \gamma\pi^0(\eta, \eta')$ are expected to proceed predominantly via two virtual gluons which subsequently convert to light hadrons, with the photon emitted from the initial charm quarks [1]. These decays provide a clean environment to study the

^{a}Also at Moscow Institute of Physics and Technology, Moscow 141700, Russia.
^{b}Also at Novosibirsk State University, Novosibirsk 630090, Russia.
^{c}Also at NRC "Kurchatov Institute," PNPI, 188300 Gatchina, Russia.
^{d}Also at Goethe University Frankfurt, 60323 Frankfurt am Main, Germany.
^{e}Also at Key Laboratory for Particle Physics, Astrophysics and Cosmology, Ministry of Education; Shanghai Key Laboratory for Particle Physics and Cosmology; Institute of Nuclear and Particle Physics, Shanghai 200240, People's Republic of China.
^{f}Also at Key Laboratory of Nuclear Physics and Ion-beam Application (MOE) and Institute of Modern Physics, Fudan University, Shanghai 200443, People's Republic of China.
^{g}Also at State Key Laboratory of Nuclear Physics and Technology, Peking University, Beijing 100871, People's Republic of China.
^{h}Also at School of Physics and Electronics, Hunan University, Changsha 410082, China.
^{i}Also at Guangdong Provincial Key Laboratory of Nuclear Science, Institute of Quantum Matter, South China Normal University, Guangzhou 510006, China.
^{j}Also at Frontiers Science Center for Rare Isotopes, Lanzhou University, Lanzhou 730000, People's Republic of China.
^{k}Also at Lanzhou Center for Theoretical Physics, Lanzhou University, Lanzhou 730000, People's Republic of China.
^{l}Also at the Department of Mathematical Sciences, IBA, Karachi 75270, Pakistan.

conversion of gluons into hadrons and to test various phenomenological mechanisms [2–6]. Of particular interest is that the study of the radiative decays of $J/\psi \to \gamma\pi^0(\eta, \eta')$ provide information on the quark composition of the η and η' mesons and the mixing between them [7–11].

Within flavor-SU(3) symmetry, the π^0, η, and η' mesons belong to the same pseudoscalar nonet. The physical states η and η' are commonly understood as mixtures of the pure SU(3)-flavor octet $[\eta_8 = (u\bar{u} + d\bar{d} - 2s\bar{s})/\sqrt{6}]$ and singlet $[\eta_1 = (u\bar{u} + d\bar{d} + s\bar{s})/\sqrt{3}]$ states,

$$\eta = \eta_8 \cos\theta_P - \eta_1 \sin\theta_P,$$
$$\eta' = \eta_8 \sin\theta_P + \eta_1 \cos\theta_P, \tag{1}$$

where θ_P is the pseudoscalar mixing angle [12]. The determination of this mixing parameter is important because it allows us to understand the properties of pseudoscalar mesons in terms of their underlying quark structure.

The radiative decays of $J/\psi \to \gamma\pi^0(\eta, \eta')$ have been studied in many experiments [13–15]. The most recent studies of $J/\psi \to \gamma\pi^0$, $J/\psi \to \gamma\eta$, and $J/\psi \to \gamma\eta'$ were reported by the BESIII Collaboration in Refs. [16–18].

In this paper, using a data sample of $(1.0087 \pm 0.0044) \times 10^{10}$ J/ψ events [19] collected by the BESIII detector, the branching fractions of $J/\psi \to \gamma\pi^0$, $J/\psi \to \gamma\eta$, and $J/\psi \to \gamma\eta'$ decays are measured. The phenomenological model-dependent mixing angles and the ratio of partial widths $\Gamma(J/\psi \to \gamma\eta')/\Gamma(J/\psi \to \gamma\eta)$ are also determined.

II. DETECTOR AND MONTE CARLO SIMULATION

The BESIII detector [20] records symmetric e^+e^- collisions provided by the BEPCII storage ring [21] in the center-of-mass energy range from 2.0 to 4.95 GeV, with a peak luminosity of 1×10^{33} cm^{-2} s^{-1} achieved at $\sqrt{s} = 3.77$ GeV. BESIII has collected large data samples in this energy region [22]. The cylindrical core of the

BESIII detector covers 93% of the full solid angle and consists of a beam pipe, a helium-based multilayer drift chamber, a plastic scintillator time-of-flight (TOF) system, and a CsI(Tl) electromagnetic calorimeter (EMC), which are all enclosed in a superconducting solenoidal magnet providing a 1.0 T (0.9 T in 2012) magnetic field. The solenoid is supported by an octagonal flux-return yoke with resistive plate counter muon identification modules interleaved with steel. The charged-particle momentum resolution at 1 GeV/c is 0.5%, and the dE/dx resolution is 6% for electrons from Bhabha scattering. The EMC measures photon energies with a resolution of 2.5% (5%) at 1 GeV in the barrel (end cap) region. The time resolution in the TOF barrel region is 68 ps, while that in the end cap region was 110 ps. The end cap TOF system was upgraded in 2015 using multigap resistive plate chamber technology, providing a time resolution of 60 ps [23].

Simulated samples produced with the GEANT4-based [24] simulation software [25], which includes the geometric description [26] of the BESIII detector and the detector response [27,28], are used to determine the detection efficiency and estimate backgrounds. The inclusive Monte Carlo (MC) sample of 1.0×10^{10} simulated inclusive J/ψ events, used to estimate the background, includes both the production of the J/ψ resonance and the continuum processes incorporated in KKMC [29]. The known decay modes are modeled with EvtGen [30] using branching fractions taken from the Particle Data Group (PDG) [31], and the remaining unknown charmonium decays are modeled with Lundcharm [32]. To estimate the selection efficiency and to optimize the selection criteria, 2.3×10^{6} MC signal events for the $J/\psi \to \gamma \pi^{0}(\eta, \eta') \to \gamma\gamma\gamma$ channels are generated, and the decay modes are described with theoretical models that have been validated in previous works [16]. The polar angle of the photon in the J/ψ center-of-mass system is defined as θ_{r}, which follows $1 + \cos^{2}\theta_{r}$ function. The analysis is performed in the framework of the BESIII off-line software system [33] which incorporates the detector calibration, event reconstruction, and data storage.

III. EVENT SELECTION AND BACKGROUND ANALYSIS

In this paper, the π^{0}, η, and η' mesons are all reconstructed via their two-photon decays. Therefore, signal events require at least three photons without any charged track in the final states.

Photon candidates are reconstructed using clusters of energy deposits in the EMC. The energy deposited in the nearby TOF system is included to improve the reconstruction efficiency and energy resolution. To exclude the background with small energy deposits in the EMC, the photon candidates are required to have an energy greater than 80 MeV in both the barrel region ($|\cos\theta| < 0.80$) and end cap regions ($0.86 < |\cos\theta| < 0.92$). A requirement on

the EMC time difference ΔT from the most energetic photon, $-500 < \Delta T < 500$ ns, is used to suppress the electronic noise and energy deposits unrelated to the event. Events with at least three photon candidates are kept for further analysis.

A four-constraint (4C) kinematic fit imposing energy and momentum conservation is performed under the hypothesis of $J/\psi \to \gamma\gamma\gamma$. If there is more than one $\gamma\gamma\gamma$ combination, the one with the smallest χ^{2}_{4C} from the kinematic fit is retained, and $\chi^{2}_{4C} < 50$ is required. To reject backgrounds from the $e^{+}e^{-} \to \gamma\gamma$ process, similar 4C kinematic fit is performed on $\gamma\gamma$ combination, χ^{2}_{4C} is required to be less than the smallest $\chi^{2}_{4C}(2\gamma)$. In the case of $J/\psi \to \gamma\pi^{0}$ decay, to suppress the background from $J/\psi \to \gamma\pi^{0}\pi^{0}$ events, in particular for events with missing low energy photons, χ^{2}_{4C} is required to be less than the smallest $\chi^{2}_{4C}(4\gamma)$, where we require only four photons to improve the efficiency. This requirement is effective in reducing 29% of $J/\psi \to \gamma\pi^{0}\pi^{0}$ background events, while removing no signal.

After the above requirements, the distribution of the two-photon invariant mass $M_{\gamma\gamma}$ is shown in Fig. 1, where the photon momenta from the 4C kinematic fit are used to calculate $M_{\gamma\gamma}$ and there are three entries per event, and the $J/\psi \to \gamma\pi^{0}\pi^{0}$ channel is shown as a peaking background for $J/\psi \to \gamma\pi^{0}$ decay.

To estimate possible backgrounds, the inclusive MC sample and the 168.30 pb^{-1} of data taken at $\sqrt{s} =$ 3.08 GeV are used [34,35]. From the inclusive MC sample, it is found that there is no peaking background for the η and η' peaks, but background events from $J/\psi \to \gamma\pi^{0}\pi^{0}$ decay form a significant peak around the nominal π^{0} mass. To estimate its contribution, a dedicated MC sample of $J/\psi \to \gamma\pi^{0}\pi^{0}$ events is produced in accordance with the partial wave analysis results [36]. Using the same selection criteria, and taking into account the number of J/ψ events
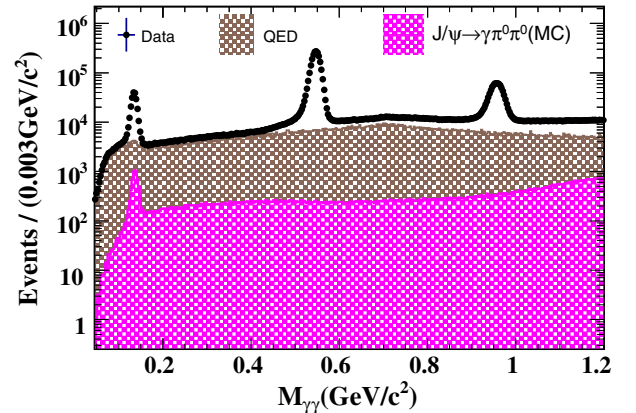

FIG. 1. The $M_{\gamma\gamma}$ distributions for data (black dots with error bars), simulated background of $J/\psi \to \gamma\pi^{0}\pi^{0}$ (pink filled area), and QED background (brown filled area). The QED background is estimated from data taken at 3.08 GeV.

and the branching fractions of $J/\psi \to \gamma\pi^0\pi^0$ [36] and $\pi^0 \to \gamma\gamma$ [31], the $M_{\gamma\gamma}$ distribution is obtained and shown as a green line in Fig. 1. The number of peaking background events in the π^0 signal region is 8208 ± 134, which is estimated by a fit to the $M_{\gamma\gamma}$ spectrum of the dedicated MC sample of $J/\psi \to \gamma\pi^0\pi^0$, where the π^0 signal is modeled with the sum of Crystal Ball (CB) [37] and Gaussian functions, while the other nonpeaking background is described with a second-order Chebyshev function.

For the background events directly from e^+e^- annihilation, the same analysis is performed on the data taken at the center-of-mass energy of 3.08 GeV. The selected events are normalized to the J/ψ data sample, after taking into account the luminosities and energy-dependent cross sections of the quantum electrodynamics (QED) processes, with a factor f

$$f \equiv \frac{N_{3.097}}{N_{3.080}} = \frac{\mathcal{L}_{3.097}}{\mathcal{L}_{3.080}} \times \frac{\sigma_{3.097}}{\sigma_{3.080}} \times \frac{\varepsilon_{3.097}}{\varepsilon_{3.080}}, \qquad (2)$$

where N, $\mathcal{L}$, σ, and ε refer to signal yields, integrated luminosities of data samples, cross sections, and detection efficiencies at the two center-of-mass energies, respectively. The details on the cross sections can be found in Ref. [38].

The normalized $M_{\gamma\gamma}$ spectrum from e^+e^- annihilation, obtained from the data at the center-of-mass energy of 3.080 GeV, is illustrated as the filled area in Fig. 1. Due to identical event topology, QED background events are indistinguishable from signal events. No obvious peaking contribution in the π^0, η, and η' signal regions is observed. Interference with the resonance amplitude is expected to be small and is ignored.

The signal yields are obtained from unbinned maximum likelihood fits to the $M_{\gamma\gamma}$ distributions in the π^0, η, and η' mass regions, as shown in Fig. 2. For each fit, the total probability density function consists of a signal and background contributions. To properly describe the data, the $\pi^0(\eta)$ signal component is modeled using a sum of CB and Gaussian functions, while the η' peak is modeled using the MC-simulated shape convoluted with a Gaussian function to account for the mass resolution difference between data and MC simulation. The background components are (i) the MC-simulated $J/\psi \to \gamma\pi^0\pi^0$ background; (ii) the QED background derived from the data taken at the center of mass of 3.08 GeV; and (iii) the other background events are parametrized with a second-order Chebyshev function. The fitted signal yields and the detection efficiencies are summarized in Table I.

IV. SYSTEMATIC UNCERTAINTIES

The systematic uncertainties of the branching fraction measurements originate mainly from the photon detection and kinematic fit efficiencies. Additional uncertainties
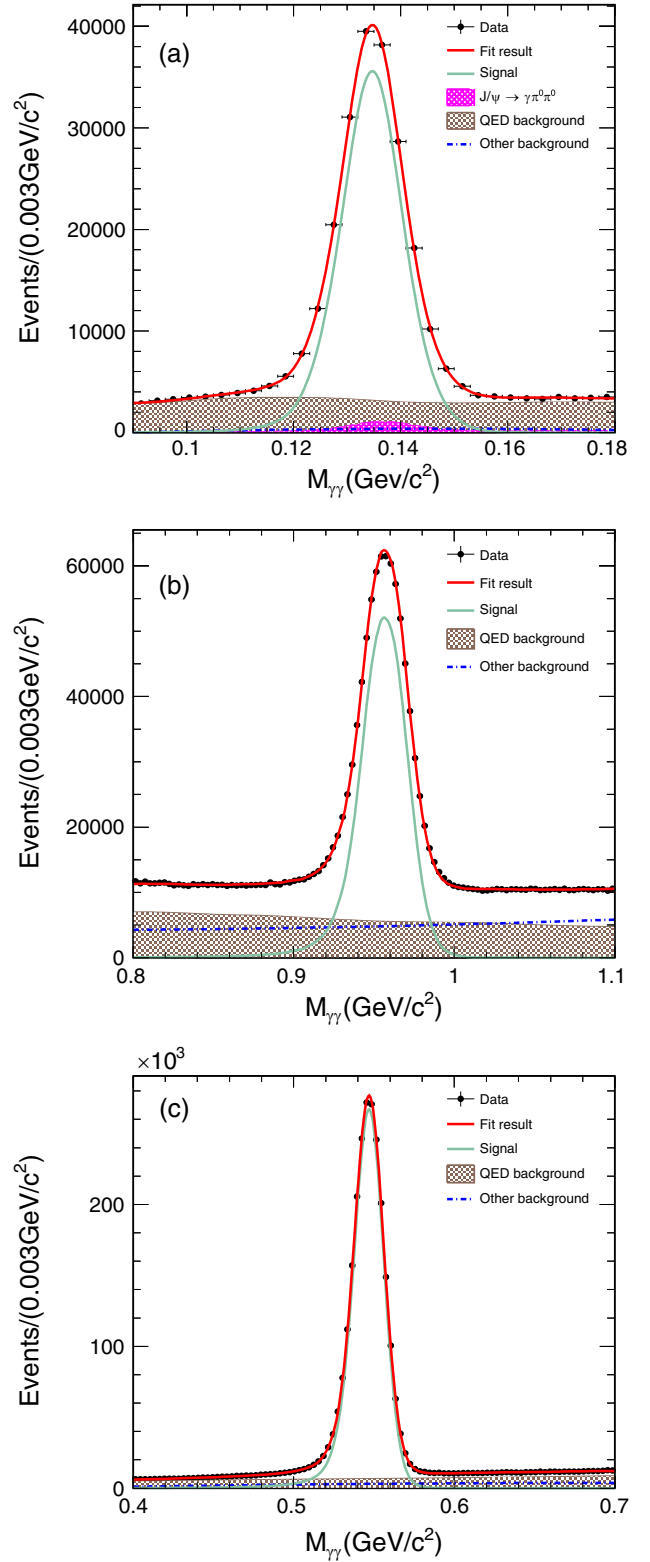

FIG. 2. The fit results of the $M_{\gamma\gamma}$ spectra for the decays of (a) $J/\psi \to \gamma\pi^0 \to 3\gamma$, (b) $J/\psi \to \gamma\eta \to 3\gamma$, and (c) $J/\psi \to \gamma\eta' \to 3\gamma$. Dots with error bars represent data, the green line represents signal, the brown filled area represents QED background, the pink filled area and blue dot-dashed line describe a contribution from $J/\psi \to \gamma\pi^0\pi^0$ and other background contributions, respectively.

TABLE I.   The branching fractions and comparison with previous results. The first uncertainty is statistical and the second is systematic. P represents the pseudoscalar meson $\pi^0(\eta, \eta')$.

| γP | $N^{\text{obs}}_{J/\psi \to \gamma P}$ | ε (%) | $\mathcal{B}(J/\psi \to \gamma P)(\times 10^{-4})$ | | |
			This work	BESIII	PDG [31]
$\gamma \pi^0$	175893 ± 839	52.90 ± 0.03	$0.334 \pm 0.002 \pm 0.009$	$0.361 \pm 0.012 \pm 0.016$ [16]	0.356 ± 0.017
$\gamma \eta$	2209063 ± 2592	50.78 ± 0.03	$10.96 \pm 0.01 \pm 0.19$	$10.67 \pm 0.05 \pm 0.23$ [17]	10.85 ± 0.18
$\gamma \eta'$	638206 ± 1061	50.77 ± 0.03	$54.0 \pm 0.1 \pm 1.1$	$52.7 \pm 0.3 \pm 0.5$ [18]	52.5 ± 0.7

associated with the fit method, signal shape, background of $J/\psi \to \gamma \pi^0 \pi^0$, QED background, branching fractions of $\pi^0(\eta, \eta') \to \gamma\gamma$, and number of J/ψ events are also considered.

A. Fit method

The uncertainty associated with the fit method comes from two sources: the fit range and background shape. The uncertainty arising from the fit range is estimated by adjusting the fit range by ± 5 MeV. The maximum differences in the branching fractions with respect to the baseline values are taken as the systematic uncertainties. To estimate the uncertainty associated with the background shape, alternative fits are performed using first- or third-order Chebyshev functions. The maximum changes of the fitted signal yields are taken as the systematic uncertainties, which are summarized in Table II.

B. Signal shape

To evaluate the systematic uncertainty arising from the signal shape, alternative fits are performed using the MC-simulated shape to describe the signal component of $J/\psi \to \gamma \pi^0(\eta)$ decays and a sum of CB and Gaussian functions for $J/\psi \to \gamma \eta'$ decay. The differences between the results with the baseline and alternative methods are taken as the corresponding systematic uncertainties.

TABLE II.   Systematic sources and corresponding contributions (%).

Source	$\gamma \pi^0$	$\gamma \eta$	$\gamma \eta'$
Fit range	0.9	0.8	1.08
Background shape	1.13	1.07	0.39
Signal shape	1.99	0.11	0.49
Background of $J/\psi \to \gamma \pi^0 \pi^0$	0.21	$\cdots$	$\cdots$
QED background	1.08	0.15	0.01
Photon detection	0.57	0.51	0.47
4C kinematic fit	0.41	0.80	0.53
Intermediate branching fractions	0.03	0.46	1.43
$N_{J/\psi}$	0.44	0.44	0.44
Total	2.82	1.77	2.07

C. Background of $J/\psi \to \gamma \pi^0 \pi^0$

The background yield of $J/\psi \to \gamma \pi^0 \pi^0$ is fixed in the fit according to the branching fraction from Ref. [36]. Alternative fits are performed varying the input branching fraction by 1 standard deviation. The biggest difference of the fitted signal yield with respect to the baseline result, 0.21%, is taken as a systematic uncertainty.

D. QED background

The QED background is estimated with Eq. (2) using the data taken at the center-of-mass energy of 3.080 GeV. Alternative fits are performed varying $\mathcal{L}_{3.080}$ in Eq. (2) by 1 standard deviation. The differences from the nominal fits are taken as the systematic uncertainties.

E. Photon detection

The systematic uncertainty of the photon detection efficiency is studied using a control sample of $e^+e^- \to \gamma\mu^+\mu^-$ events. The four-momentum of the initial-state-radiation photon is predicted by the $\mu^+\mu^-$ pair. The photon detection efficiency is defined as the fraction of reconstructed photons with four-momentum matching in the EMC. The systematic uncertainty is defined as the relative difference in efficiency between data and MC simulation, which is estimated using a reweighting technique [39]. The uncertainties of the photon detection for the $J/\psi \to \gamma \pi^0$, $J/\psi \to \gamma \eta$, and $J/\psi \to \gamma \eta'$ decays are 0.57%, 0.51%, and 0.47%, respectively.

F. Kinematic fit

The uncertainty of the kinematic fit mainly comes from the inconsistency of the photon resolution between data and MC simulation. We adjust the energy resolution in the reconstructed photon error matrix so that the MC simulation provides a good description of data [40]. The fits are redone, and the changes with respect to the nominal results are taken as the systematic uncertainties.

G. Intermediate branching fractions

The branching fractions of intermediate decays are taken from the PDG [31]. The uncertainties of the branching

fractions of $\pi^0 \to \gamma\gamma$, $\eta \to \gamma\gamma$, and $\eta' \to \gamma\gamma$ are 0.03%, 0.46%, and 1.43%, respectively.

H. Number of J/ψ events

The number of J/ψ events is determined to be $(1.0087 \pm 0.0044) \times 10^{10}$ using inclusive hadronic J/ψ decays [19]. Its uncertainty, 0.44%, is taken as a systematic uncertainty.

The systematic uncertainties are summarized in Table II. The total systematic uncertainty is given by the square root of the quadratic sum of the individual contributions.

V. RESULTS

The branching fraction of $J/\psi \to \gamma P$ is calculated as

$$\mathcal{B}(J/\psi \to \gamma P) = \frac{N_{\mathrm{obs}}}{N_{J/\psi} \times \mathcal{B}(P \to \gamma\gamma) \times \varepsilon}, \qquad (3)$$

where P represents the pseudoscalar meson $\pi^0(\eta, \eta')$, N_{obs} is the number of the observed signal events, $N_{J/\psi}$ is the number of J/ψ events, ε is the detection efficiency, and $\mathcal{B}(P \to \gamma\gamma)$ is the branching fraction of $P \to \gamma\gamma$ [31].

The measured branching fractions using Eq. (3) are summarized in Table I. They are in agreement with the previous BESIII results [16–18] and the world average values [31]. The results allow the study of pseudoscalar mixing in Eq. (1). Under the assumption of exact SU(3)-flavor symmetry, the mixing angle can be determined via

$$R = \frac{\Gamma(J/\psi \to \gamma\eta')}{\Gamma(J/\psi \to \gamma\eta)} = \left(\frac{p_{\eta'}}{p_\eta}\right)^3 \cdot \cot^2 \theta_P, \qquad (4)$$

where p_η and $p_{\eta'}$ are the momenta of η and η' in the J/ψ rest frame, respectively. The systematic uncertainties caused by the number of J/ψ events and photon detection efficiency can be eliminated in the ratio calculation. According to the theoretical calculation [8], the θ_P value is negative. Finally, we obtain $\theta_P = -(22.11 \pm 0.26)°$, where the uncertainty includes both statistical and systematic uncertainties.

The $\eta - \eta'$ mixing approach has been generalized to also include other states, such as π^0 meson. The decay width of $J/\psi \to \gamma P$ is given by [41]

$$\Gamma(J/\psi \to \gamma P) = \frac{1}{3} \frac{g_{\gamma P}^2}{4\pi} \frac{p^3}{m_{J/\psi}^2}, \qquad (5)$$

where $g_{\gamma P}^2$ is the coupling constant defined by the amplitude, as shown in Table III, and p is the magnitude of momentum of P. In this table, d and f coefficients are free parameters, derived from a joint set of decay width equations, which cancel in the calculation, and the details can be found in the Appendix. The $X_{\eta(\eta')}$ and $Y_{\eta(\eta')}$ are related to the following:

TABLE III.   Amplitudes for the decays of $J/\psi \to \gamma P$.

Decay mode	Amplitude
$\gamma\pi^0$	$\frac{f}{\sqrt{6}}$
$\gamma\eta$	$\frac{2}{\sqrt{6}}(d + \frac{f}{3})X_\eta + \frac{1}{\sqrt{3}}(d - \frac{f}{3})Y_\eta$
$\gamma\eta'$	$\frac{2}{\sqrt{6}}(d + \frac{f}{3})X_{\eta'} + \frac{1}{\sqrt{3}}(d - \frac{f}{3})Y_{\eta'}$

$$X_\eta = Y_{\eta'} = \cos\theta_P/\sqrt{3} - \sqrt{\frac{2}{3}}\sin\theta_P,$$

$$Y_\eta = -X_{\eta'} = -\sqrt{\frac{2}{3}}\cos\theta_P - \sin\theta_P/\sqrt{3}. \qquad (6)$$

The θ_P value is determined to be $-(19.34 \pm 0.34)°$, where the uncertainty includes both statistical and systematic uncertainties.

VI. SUMMARY

Based on $(1.0087 \pm 0.0044) \times 10^{10}$ J/ψ events collected with the BESIII detector, a study of $J/\psi \to \gamma\pi^0(\eta, \eta')$ decays is performed. The branching fractions of $J/\psi \to \gamma\pi^0$, $J/\psi \to \gamma\eta$, and $J/\psi \to \gamma\eta'$ are measured to be $(3.34 \pm 0.02 \pm 0.09) \times 10^{-5}$, $(1.096 \pm 0.001 \pm 0.019) \times 10^{-3}$, and $(5.40 \pm 0.01 \pm 0.11) \times 10^{-3}$, respectively, which are consistent with the previous measurements [13,14,16–18] within 2 standard deviations. As shown in Table I, the result for $B(J/\psi \to \gamma\pi^0)$ has much better precision compared with the previous BESIII result, while $B(J/\psi \to \gamma\eta)$ also has better precision. With two phenomenological models [42], the singlet-octet pseudoscalar mixing angles of θ_P are determined to be $\theta_P = -(22.11 \pm 0.26)°$ and $-(19.34 \pm 0.34)°$, respectively, which are consistent with the theoretical calculation of Refs. [8,9].

APPENDIX: CALCULATION OF θ_P

The decay width of $J/\psi \to \gamma P$ is given by Eq. (5). One can obtain that

$$\frac{\Gamma(J/\psi \to \gamma\eta)}{\Gamma(J/\psi \to \gamma\pi^0)} = \frac{g_{\gamma\eta}^2}{g_{\gamma\pi^0}^2}\frac{p_\eta^3}{p_{\pi^0}^3} = \frac{\mathcal{B}(J/\psi \to \gamma\eta)}{\mathcal{B}(J/\psi \to \gamma\pi^0)}, \quad \text{(A1)}$$

$$\frac{\Gamma(J/\psi \to \gamma\eta')}{\Gamma(J/\psi \to \gamma\pi^0)} = \frac{g_{\gamma\eta'}^2}{g_{\gamma\pi^0}^2}\frac{p_{\eta'}^3}{p_{\pi^0}^3} = \frac{\mathcal{B}(J/\psi \to \gamma\eta')}{\mathcal{B}(J/\psi \to \gamma\pi^0)}, \quad \text{(A2)}$$

where $g_{\gamma P}^2$ is the coupling constant defined by the amplitude, as shown in Table III, and p is the magnitude of momentum of P. Then we have

$$\sqrt{\frac{\mathcal{B}(J/\psi \to \gamma\eta)}{\mathcal{B}(J/\psi \to \gamma\pi^0)}\frac{p_{\pi^0}^3}{p_\eta^3}} = \frac{g_{\gamma\eta}}{g_{\gamma\pi^0}} = \frac{\frac{2}{\sqrt{6}}(d+\frac{f}{3})X_\eta + \frac{1}{\sqrt{3}}(d-\frac{f}{3})Y_\eta}{\frac{f}{\sqrt{6}}}$$

$$= \frac{\frac{2}{\sqrt{6}}(d+\frac{f}{3})\left(\cos\theta_P/\sqrt{3} - \sqrt{\frac{2}{3}}\sin\theta_P\right) + \frac{1}{\sqrt{3}}(d-\frac{f}{3})\left(-\sqrt{\frac{2}{3}}\cos\theta_P - \sin\theta_P/\sqrt{3}\right)}{\frac{f}{\sqrt{6}}}$$

$$= \frac{-9\sqrt{2}d\sin\theta_P + 4f\cos\theta_P - \sqrt{2}f\sin\theta_P}{3\sqrt{3}f}, \quad \text{(A3)}$$

$$3\sqrt{3}f\cos\theta_P\sqrt{\frac{\mathcal{B}(J/\psi \to \gamma\eta)}{\mathcal{B}(J/\psi \to \gamma\pi^0)}\frac{p_{\pi^0}^3}{p_\eta^3}} = -9\sqrt{2}d\sin\theta_P\cos\theta_P + 4f\cos^2\theta_P - \sqrt{2}f\sin\theta_P\cos\theta_P, \quad \text{(A4)}$$

$$\sqrt{\frac{\mathcal{B}(J/\psi \to \gamma\eta')}{\mathcal{B}(J/\psi \to \gamma\pi^0)}\frac{p_{\pi^0}^3}{p_{\eta'}^3}} = \frac{g_{\gamma\eta'}}{g_{\gamma\pi^0}} = \frac{\frac{2}{\sqrt{6}}(d+\frac{f}{3})X'_\eta + \frac{1}{\sqrt{3}}(d-\frac{f}{3})Y'_\eta}{\frac{f}{\sqrt{6}}}$$

$$= \frac{\frac{2}{\sqrt{6}}(d+\frac{f}{3})\left(\sin\theta_P/\sqrt{3} + \sqrt{\frac{2}{3}}\cos\theta_P\right) + \frac{1}{\sqrt{3}}(d-\frac{f}{3})\left(-\sqrt{\frac{2}{3}}\sin\theta_P + \cos\theta_P/\sqrt{3}\right)}{\frac{f}{\sqrt{6}}}$$

$$= \frac{9\sqrt{2}d\cos\theta_P + 4f\sin\theta_P + \sqrt{2}f\cos\theta_P}{3\sqrt{3}f}, \quad \text{(A5)}$$

$$3\sqrt{3}f\sin\theta_P\sqrt{\frac{\mathcal{B}(J/\psi \to \gamma\eta')}{\mathcal{B}(J/\psi \to \gamma\pi^0)}\frac{p_{\pi^0}^3}{p_{\eta'}^3}} = 9\sqrt{2}d\sin\theta_P\cos\theta_P + 4f\sin^2\theta_P + \sqrt{2}f\sin\theta_P\cos\theta_P. \quad \text{(A6)}$$

With Eqs. (A4) and (A6), one can obtain that

$$3\sqrt{3}f\cos\theta_P\sqrt{\frac{\mathcal{B}(J/\psi \to \gamma\eta)}{\mathcal{B}(J/\psi \to \gamma\pi^0)}\frac{p_{\pi^0}^3}{p_\eta^3}} + 3\sqrt{3}f\sin\theta_P\sqrt{\frac{\mathcal{B}(J/\psi \to \gamma\eta')}{\mathcal{B}(J/\psi \to \gamma\pi^0)}\frac{p_{\pi^0}^3}{p_{\eta'}^3}} = 4f(\sin^2\theta_P + \cos^2\theta_P), \quad (A7)$$

$$\frac{3\sqrt{3}}{4}\cos\theta_P\sqrt{\frac{\mathcal{B}(J/\psi \to \gamma\eta)}{\mathcal{B}(J/\psi \to \gamma\pi^0)}\frac{p_{\pi^0}^3}{p_\eta^3}} + \frac{3\sqrt{3}}{4}\sin\theta_P\sqrt{\frac{\mathcal{B}(J/\psi \to \gamma\eta')}{\mathcal{B}(J/\psi \to \gamma\pi^0)}\frac{p_{\pi^0}^3}{p_{\eta'}^3}} = 1. \quad (A8)$$

Equation (A9) can be written as

$$X\cos\theta_P + Y\sin\theta_P = 1, \quad (A9)$$

where $X = \frac{3\sqrt{3}}{4}\sqrt{\frac{\mathcal{B}(J/\psi\to\gamma\eta)}{\mathcal{B}(J/\psi\to\gamma\pi^0)}\frac{p_{\pi^0}^3}{p_\eta^3}}$, $Y = \frac{3\sqrt{3}}{4}\sqrt{\frac{\mathcal{B}(J/\psi\to\gamma\eta')}{\mathcal{B}(J/\psi\to\gamma\pi^0)}\frac{p_{\pi^0}^3}{p_{\eta'}^3}}$. Then,

$$\begin{aligned}
X\sin\theta_P - Y\cos\theta_P &= \pm\sqrt{X^2\sin^2\theta_P + Y^2\cos^2\theta_P - 2XY\sin\theta_P\cos\theta_P} \\
&= \pm\sqrt{X^2\sin^2\theta_P + Y^2\cos^2\theta_P - [(X\cos\theta_P + Y\sin\theta_P)^2 - (X^2\cos^2\theta_P + Y^2\sin^2\theta_P)]} \\
&= \pm\sqrt{X^2(\sin^2\theta_P + \cos^2\theta_P) + Y^2(\sin^2\theta_P + \cos^2\theta_P) - 1} \\
&= \pm\sqrt{X^2 + Y^2 - 1}.
\end{aligned} \quad (A10)$$

According to Eqs. (A10) and (A11), one can obtain that

$$\begin{cases} X\cos\theta_P + Y\sin\theta_P = 1 \\ X\sin\theta_P - Y\cos\theta_P = \pm\sqrt{X^2 + Y^2 - 1}, \end{cases} \quad (A11)$$

$$\begin{cases} Y(X\cos\theta_P + Y\sin\theta_P) = Y \\ X(X\sin\theta_P - Y\cos\theta_P) = \pm X\sqrt{X^2 + Y^2 - 1}, \end{cases} \quad (A12)$$

$$(X^2 + Y^2)\sin\theta_P = Y \pm X\sqrt{X^2 + Y^2 - 1}, \quad (A13)$$

$$\sin\theta_P = \frac{Y \pm X\sqrt{X^2 + Y^2 - 1}}{X^2 + Y^2}. \quad (A14)$$

According to the theoretical calculation of Ref. [8], the value of θ_P is negative,

$$\theta_P = \arcsin\left(\frac{Y - X\sqrt{X^2 + Y^2 - 1}}{X^2 + Y^2}\right). \quad (A15)$$

[1] Norikazu Morisita, Ichijiro Kitamura, and Tadayuki Teshima, Phys. Rev. D **44**, 175 (1991).

[2] V. L. Chernyak and A. R. Zhitnitsky, Phys. Rep. **112**, 173 (1984).

[3] J. G. Körner *et al.*, Nucl. Phys. **B229**, 115 (1983).

[4] G. W. Intemann, Phys. Rev. D **27**, 2755 (1983).

[5] H. Fritzsch and J. D. Jackson, Phys. Lett. B **66B**, 365 (1977).

[6] K. T. Chao, Nucl. Phys. **B335**, 101 (1990).

[7] J. L. Rosner, Phys. Rev. D **27**, 1101 (1983); *Proceedings of the 1985 International Symposium on Lepton and Photon Interactions at High Energies, Kyoto, Japan, 1985*, edited by M. Konuma and K. Takahashi (Research Institute of Fundamental Physics, Kyoto University, Kyoto, 1986), p. 448.

[8] F. J. Gilman and R. Kauffman, Phys. Rev. D **36**, 2761 (1987); **37**, 3348(E) (1988).

[9] Xiangyu Jiang, Feiyu Chen, Ying Chen, Ming Gong, Ning Li, Zhaofeng Liu, Wei Sun, and Renqiang Zhang, Phys. Rev. Lett. **130**, 061901 (2023).

[10] K. Kawarabayashi and N. Ohta, Nucl. Phys. **B175**, 477 (1980).

[11] K. Kawarabayashi and N. Ohta, Prog. Theor. Phys. **66**, 1709 (1981).

[12] J. F. Donoghue, B. R. Holstein, and Y.-C. R. Lin, Phys. Rev. Lett. **55**, 2766 (1985); R. Escribano and J.-M. Frère, J. High Energy Phys. 06 (2005) 029.

[13] M. Ablikim *et al.* (BES Collaboration), Phys. Rev. D **73**, 052008 (2006).

[14] T. K. Pedlar *et al.* (CLEO Collaboration), Phys. Rev. D **79**, 111101(R) (2009).

[15] M. Ablikim *et al.* (BES Collaboration), Phys. Rev. D **83**, 012003 (2011).

[16] M. Ablikim *et al.* (BESIII Collaboration), Phys. Rev. D **97**, 072014 (2018).

[17] M. Ablikim *et al.* (BESIII Collaboration), Phys. Rev. D **104**, 092004 (2021).

[18] M. Ablikim *et al.* (BESIII Collaboration), Phys. Rev. Lett. **122**, 142002 (2019).

[19] M. Ablikim *et al.* (BESIII Collaboration), Chin. Phys. C **46**, 074001 (2022).

[20] M. Ablikim *et al.* (BESIII Collaboration), Nucl. Instrum. Methods Phys. Res., Sect. A **614**, 345 (2010).

[21] C. H. Yu *et al.*, in *Proceedings of IPAC2016, Busan, Korea* (2016), 10.18429/JACoW-IPAC2016-TUYA01.

[22] M. Ablikim *et al.* (BESIII Collaboration), Chin. Phys. C **44**, 040001 (2020).

[23] X. Li *et al.*, Radiat. Detect. Technol. Methods **1**, 13 (2017); Y. X. Guo *et al.*, Radiat. Detect. Technol. Methods **1**, 15 (2017); P. Cao *et al.*, Nucl. Instrum. Methods Phys. Res., Sect. A **953**, 163053 (2020).

[24] S. Agostinelli *et al.* (GEANT4 Collaboration), Nucl. Instrum. Methods Phys. Res., Sect. A **506**, 250 (2003).

[25] Z. Y. Deng *et al.*, Chin. Phys. C **30**, 371 (2006).

[26] K. X. Huang *et al.*, Nucl. Sci. Tech. **33**, 142 (2022).

[27] Y. T. Liang, B. Zhu, Z. Y. You *et al.*, Nucl. Instrum. Methods Phys. Res., Sect. A **603**, 325 (2009).

[28] Z. Y. You, Y. T. Liang, and Y. J. Mao, Chin. Phys. C **32**, 572 (2008).

[29] S. Jadach, B. F. L. Ward, and Z. Was, Phys. Rev. D **63**, 113009 (2001).

[30] D. J. Lange, Nucl. Instrum. Methods Phys. Res., Sect. A **462**, 152 (2001); R. G. Ping, Chin. Phys. C **32**, 599 (2008).

[31] R. L. Workman *et al.* (Particle Data Group), Prog. Theor. Exp. Phys. **2022**, 083C01 (2022).

[32] J. C. Chen, G. S. Huang, X. R. Qi, D. H. Zhang, and Y. S. Zhu, Phys. Rev. D **62**, 034003 (2000); R. L. Yang, R. G. Ping, and H. Chen, Chin. Phys. Lett. **31**, 061301 (2014).

[33] J. Zhang *et al.*, Radiat. Detect. Technol. Methods **2**, 20 (2018).

[34] M. Ablikim *et al.* (BESIII Collaboration), Chin. Phys. C **41**, 013001 (2017).

[35] M. Ablikim *et al.* (BESIII Collaboration), Chin. Phys. C **46**, 074001 (2022).

[36] M. Ablikim *et al.* (BESIII Collaboration), Phys. Rev. D **92**, 052003 (2015).

[37] J. H. Cheng, Z. Wang, L. Lebanowski, G.-L. Lin, and S. Chen, Nucl. Instrum. Methods Phys. Res., Sect. A **827**, 165 (2016).

[38] J. M. Bian *et al.*, Int. J. Mod. Phys. A **24**, 267 (2009).

[39] D. Martschei, M. Feindt, S. Honc, and J. Wagner-Kuhr, J. Phys. Conf. Ser. **368**, 012028 (2012).

[40] M. Ablikim *et al.* (BESIII Collaboration), Phys. Rev. Lett. **130**, 081901 (2023).

[41] Norikazu Morisita, Ichijiro Kitamura, and Tadayuki Teshima, Phys. Rev. D **44**, 175 (1991).

[42] R. N. Cahn and M. S. Chanowitz, Phys. Lett. **59B**, 277 (1975).